Development of thermal runaway emissions aftertreatment system (TREAS) of lithium ion batteries

Daniel Darnikowski*[1,2]

[1] *Maritime Advanced Research Centre, Szczecińska 65, 80-392 Gdańsk, Poland*
[2] *Institute of Fluid-Flow Machinery, Polish Academy of Sciences*
14 Fiszera Street, 80-231, Gdansk, Poland

Abstract

Lithium-ion batteries are one of the most cost effective portable energy containers. The fire incident involving such battery (often referred as "thermal runaway"), however, poses a great danger to the surrounding, particularly in the matter of emitted substances and their toxicity for human body. The substances found are carbon monoxide and dioxide, hydrogen and hydrogen fluoride. Filtration of these substances may be achieved with dry sorbent injection method, which uses calcium hydroxide. Dry injection filtering prototype is manufactured and tested against thermal runaway of the NCM cells. Following parameters are analysed: air flow, sorbet transport, air temperature of the flue gas and concentrations of the substances. Estimated filtering performance of the dry sorbent injection and air dilution at a flow rate of 1600 m^3/h and dosage of 1.8 g/s of calcium hydroxide is 99% for HF and 89% for CO_2. NMC cell gas production per Wh were respectively 1060.3 mg of CO_2 and 11.8 mg of H_2. Air speed of above 5 m/s was found sufficient to transfer the sorbent power from the hopper's inlet.

Keywords: lithium-ion, after-treatment, thermal runaway, emissions, LIB

1 Introduction

Lithium-ion batteries (LIB) are an enormous achievement in terms of technical and commercial side. LIB allows a vast scale of applications ranging from the cellphones to the large scale battery energy storage systems. Simultaneously, the fire caused by lithium-ion batteries are of a great concern, due to intense heat production as well as emissions of toxic gases [1–5]. Heat generated by the fire is a serious threat itself, however, toxic fumes may be even of a greater consideration, especially in a confined spaces such as closed rooms, underground parking spaces, spacecrafts, airplanes and other.

The fire incident of lithium-ion battery is caused by the event called "thermal runaway". Thermal runaway is a process that is accelerated by increased temperature, in turn releasing energy that further increases temperature [6]. In terms of lithium-ion battery (LIB), one or multiple cells start releasing internal energy in form of heat, which

*Corresponding Author. Email address: daniel.darnikowski@cto.gda.pl
https://doi.org/10.58139/v2q1-r455

is then transferred to another cells and modules causing a cascading effect [7, 8]. The initiation of the thermal runaway can have different causes - they are usually divided into three sources - mechanical abuse - such as in a crash, thermal abuse - e.g. overheating of the batteries or exposure to external source of heat or electrical abuse - e.g. overcharging. Summary of thermal runway mechanism has been shown in Fig. 1.

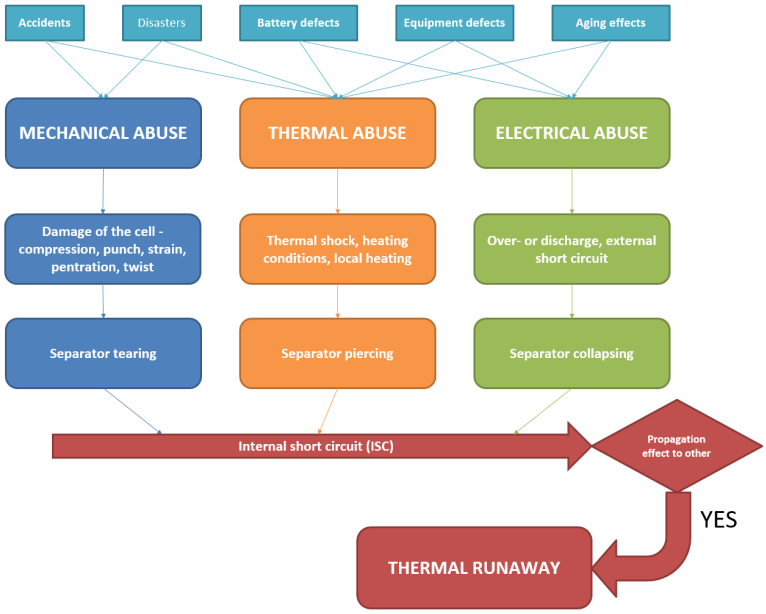

Figure 1: Battery safety issues. First row represents potential causes for LIB abuse. Second row divides given incident due to type of the abuse. Third row presents the examples of the processes causing given abuse to which LIBs are subjected. Fourth row presents damage to separator, which then results in internal short circuit [9]

.

Thermal runaway poses great challenge to the fire fighting brigades due to their self-sustaining nature [10], enclosures of the batteries inhibiting an easy pass of the cooling agent, toxic gaseous emissions [11] and heat generation [12]. The battery cannot be doused with conventional methods, as the battery is able to produce the oxygen by itself [11]. Instead, a lithium-ion battery is extinguished usually with the combination of state-of-art technology allowing to penetrate the enclosure battery with the cooling agents and then to drop the temperature below the critical point [13].

Since lithium-ion batteries cause severe incidents, which are difficult to control, they must undertake series of abuse tests before their introduction to the market [9, 14]. Type approval tests differ depending on geographical location of their the approving body [15], however, tests concerning fire resistance or exposure to high temperature usually cause test specimen to undergo thermal runaway event, producing vast amount of toxic compounds such as hydrogen fluoride, carbon monoxide, hydrogen, benzine and other cancerous aromatic compounds [16] and greenhouse gases [1]. Testing procedures such as GTR 20:2018 [17] (China), UNECE R100.02:2013 [18] (Europe), UN-ECE R100.03:2021 [19], ISO 12405-3:2014 [20] (global), ISO 6469-1:2019 [21] (global), ISO 18243:2017 [22] (global), SAE J2464:2009 [23] (North America), GB/T 31467.3-

2015 [24] (China), SAND2017-6925:2017 [25] (North America) and UL 2580:2020 [26] (North America) either deliberately cause thermal runaway to test against any signs of explosion of the cell, module or battery pack or use external heat source (petrol) to induce it.

Due to the fact there is little provided data on the methods of cleaning the toxic gases coming from the thermal runaway of the lithium-ion batteries, this paper describes the development of such prototype device together with the review of the compounds found in emitted gases, chemical and mechanical modelling of the device and test results containing air flow measurements and chemical analysis.

2 Thermal runaway emissions of lithium-ion batteries

Thermal runaway is preceded by the increase of temperature of the lithium-ion cell. First step is a breakdown of SEI layer (solid electrolyte interphase layer), layered on the anode. SEI layer purpose is to protect the anode from further reacting with the electrolyte [27]. The breakdown of the thin SEI layer occurs at 90-120°C, producing primarily CO_2 [28]:

$$(CH_2OCO_2Li)_2 \longrightarrow Li_2CO_3 + C_2H_4 + CO_2 + \tfrac{1}{2}\,O_2$$

Subsequently, due to SEI layer decomposition anode and electrolyte start to interact. Typical electrolytes found in lithium-ion batteries and their reaction with anode form flammable hydrocarbons are shown below [29]:

$$2\,Li + C_3H_4O_3\,(EC) \longrightarrow Li_2CO_3 + C_2H_4$$
$$2\,Li + C_4H_6O_3\,(PC) \longrightarrow Li_2CO_3 + C_3H_6$$
$$2\,Li + C_3H_6O_3\,(DMC) \longrightarrow Li_2CO_3 + C_2H_6$$

Subsequently, polyethylene or polypropylene separator melts at 135°C and 166°C respectively, and ceramic coated separator is found to maintain integrity even over 200°C [30]. As the temperature increase the separator shrinks until cathode and anode come into contact with each other to induce internal short circuit (ISC). ISC is a precursor for a thermal runaway, electric energy stored in the cell is further released in the approximately same amount [31].

Further reactions depend on the type of cathode used in the cell. These reaction mainly produce metallic oxides such as Co_3O_4 for LCO [32], LixCOyAlzOp for NCA, $(Mn, Ni)O$ and $Lix(Ni_{1/3}Co_{1/3}Mn_{1/3})O_2$ for NCM [33, 34] and other. Additionally, other by-products include oxygen and solid state metals.

Together with the cathode decomposition, electrolyte used in battery cell emits particular amount and type of toxic compounds. It is flammable and usually contains lithium hexafluorophosphate ($LiPF_6$) or other Li-based salts containing fluorine [35]. Promoted by the presence of water and humidity following reactions constitute to electrolyte decomposition [16]:

$$LiPF_6 \longrightarrow LiF + PF_6$$
$$PF_5 + H_2O \longrightarrow POF_3 + 2\,HF$$
$$LiPF_6 + H_2O \longrightarrow LiF + POF_3 + 2\,HF$$

The data has shown the production of HF and PO_3 per Wh at 100% SOC can be up to 193.3 mg and 22 mg respectively [16]. The production of other gaseous substances

is dependent on the state of charge as well as type of chemistry used in the cell [36] and Fig. 2. Total gas generation is largely varying on used cathode material, state of charge of the cell and its shape. For the LCO/NCM 18650 type cell, it was found to be 265 mmol [37].

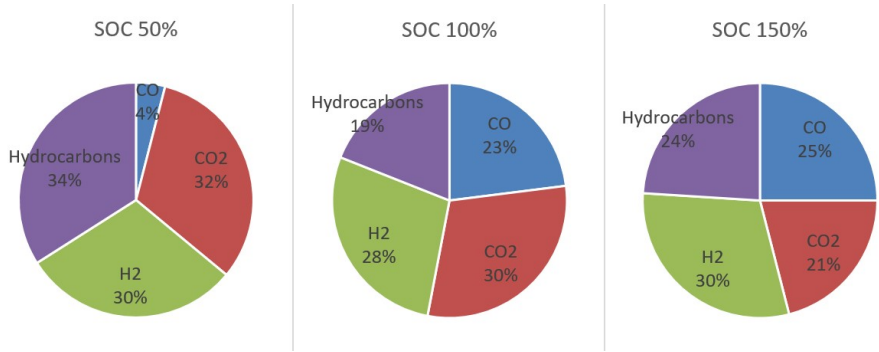

Figure 2: Composition of gases generated from thermal runaway of commercial LIBs. Somendepalli et al. [36] results of gas generated from 7.7 Wh LCO cell at different SOC.

3 Cleaning methods of the gas emissions

Toxic and acid gases, such as HCl, SO_2, CO_2, CO and HF can be neutralized by the designed agents, either supplied by the wet scrubbing equipment in absorbent solutions or by dry injection systems such as powdered alkaline sorbents [38]. Dry sorbent injection (DSI) systems characterise with low installed capital costs, relatively easy to retrofit to a majority of facilities, the system ensures good flexibility for various sorbents and low consumable requirements as well as parasitic power requirements to operate [39]. The two compounds have been predominantly used in the DSI - sodium or calcium-based [38, 40] - with the latter emerging as more accessible due to general availability of the limestone (calcium hydroxide) [41]. As such, calcium hydroxide was chosen for the TREAS to primarily clean hydrogen fluoride emissions.

After the calcium hydroxide is injected into gas emissions containing HF and CO_2 the following reactions can occur:

$$Ca(OH)_2 + 2\,HF \longrightarrow CaF_2 + H_2O$$

$$Ca(OH)_2 + CO_2 \longrightarrow CaCO_3 + H_2O$$

Thermodynamic calculations show the $CaCO_3$ and CaF_2 can only be formed at the temperatures below 600-800°C [42]. The products of reaction of the dry sorbent injection are then removed with mechanical filters (bag filters) and transposed to waste. The filter is intermittently cleaned with the jet pulse of air aimed. The schematics for the Thermal Runaway Emissions Aftertreatment System using dry sorbent injection are shown in Fig. 3.

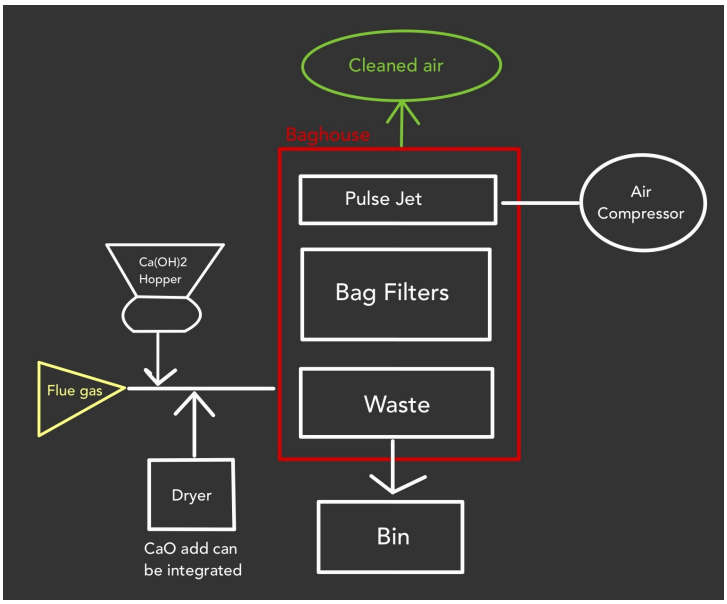

Figure 3: TREAS schematics using dry sorbent injection and calcium hydroxide. From right to left: flue gas is collected by the use of extraction hood, transported through the ventilation pipes to the baghouse. In midway the calcium hydroxide hopper supplies a dry sorbent in form of powder; dryer is optional. The bag house consists of mechanical filter (bag filter), air pulse jet (a nozzle to release compressed air for bag filter cleaning) and waste funnel (cone-shaped to limit the air leakage), below the baghouse a bin collects used dry sorbent agent. Other devices were air compressor for the pulse jet and fan for air flow with extraction of gases.

4 Development and test results of TREAS

Thermal Runaway Emissions Aftertreatment System was developed in stages with the optimisation of the air flow with the use of 3D modelling (Siemens NX), CFD computations (SOLIDWORKS Flow Simulation) and measurements on prototype and testing of thermal runaway NCM cells in various configurations. Next chapters present subsequent steps in TREAS development process.

The prototype is shown in Fig. 4.

4.1 Air flow simulations and measurements of the TREAS

The air flow in TREAS was simulated with SOLIDWORKS Flow Simulation CFD software. Nine TREAS 3D models were tested with various connectors and joints being used at 50°C and 300°C and with the fan performance of 1500 m^3/h. The model presumed the bottom outlet for the sorbent waste was closed for the sake of simulation simplicity. The overall pressure drops were respectively 300.9 Pa and 171.4 Pa for 50 and 300°C. The final model was shown in Fig. 5. The air flow before the filter bag were calculated to be at about 13 m/s, which were deemed optimal for the filtration purposes.

Figure 4: TREAS prototype testing site. P1, P2 and P3 probing points of the air flow. T1, T2, T3 temperature measurement points.

The measurement of the air flow was made on the TREAS prototype with the use of TESTO 480 anemometer and 0635 hot-wire probe. The probing was made in three locations shown in Fig. 4 and two fan performances (at 80% and 90%) for 30 min. and 1 Hz sampling:

- P1 - probing point after the fan.
- P2 - probing point before the filter.
- P3 - probing point at the extraction hood inlet.

The results of the flow measurement are shown in Fig. 6. The wind speed at the extraction hood inlet (P3) and before the filter (P2) is respectively 5 and 2-times lower than the simulated. It was found this is caused attributable to air leakages of the dosing system and waste removal. Simultaneously, the air flow was deemed sufficient to provide the transport and mixing of the dry sorbent, allow for periodical waste removal (jet-pulse), as well as limit the temperature of the thermal runaway gases, which may cause the filter to disintegrate. The wind speed at the fan exhaust was found similar to the simulated results.

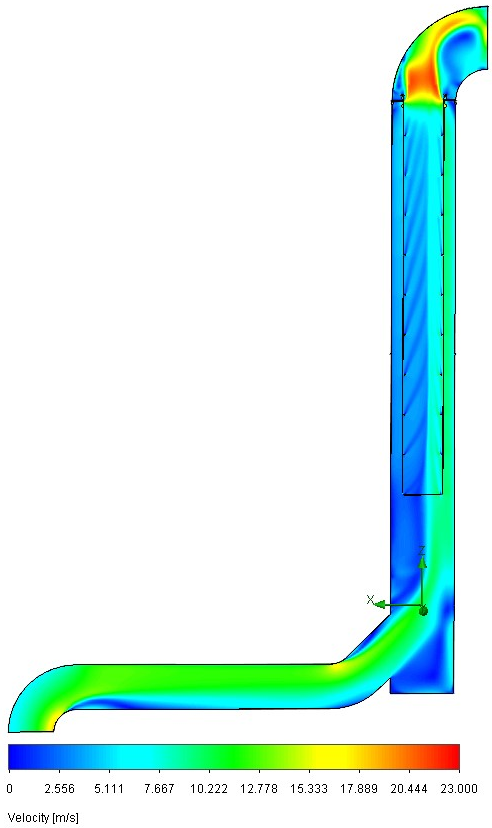

Figure 5: TREAS final model simulation at 50°C and 1500 m^3/h.

4.2 Thermal runaway tests

A series of tests were prepared to test the prototype performance in terms of gaseous composition (carbon dioxide, hydrogen and hydrogen fluoride) and temperature distribution inside TREAS. For the gas analysis a IR carbon dioxide sensor (resolution 0-100% v/v) and electrochemical sensors for hydrogen (resolution 0-40000 ppm v/v) and hydrogen fluoride (resolution 0-10 ppm v/v). Following configurations were tested two times each:

- Test Set-up 1: Thermal runaway of one NCM pouch battery cell (3.7 V, 60Ah, 220 Wh, 300x180x12 mm, 1120 g), fan power at 80%, sorbent dosage 1.8 g/s, pulse jet interval - 45 s break with 2 s air jet pulse.
- Test Set-up 2: Thermal runaway of two NCM pouch battery cell (3.7 V, 60Ah, 220 Wh, 300x180x12 mm, 1120 g), fan power at 90%, sorbent dosage 1.8 g/s, pulse jet interval - 45 s break with 2 s air jet pulse.
- Test Set-up 3: Thermal runaway of one NCM pouch battery cell (3.7 V, 60Ah, 220 Wh, 300x180x12 mm, 1120 g), fan power at 80%, sorbent dosage 0 g/s, pulse jet interval - off.

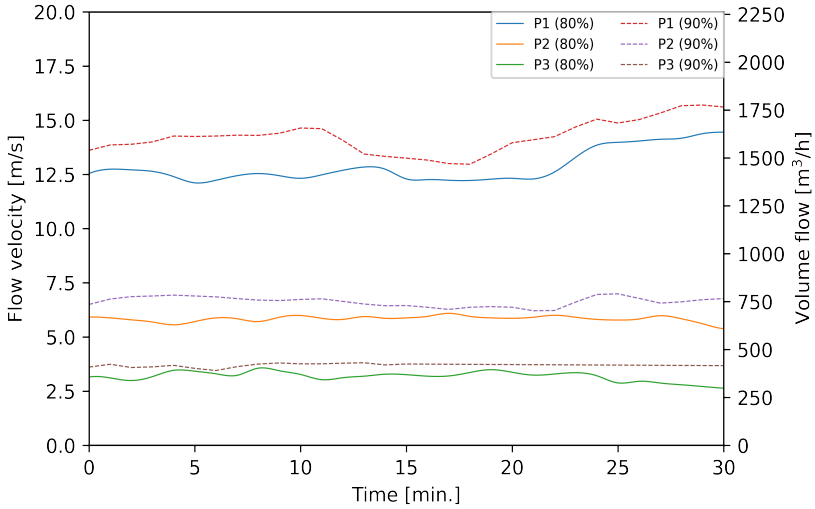

Figure 6: Flow measurements of the TREAS prototype at an ambient temperature and two fan performances. P1, P2 and P3 probing points of the air flow, see Fig. 4.

Table 1: Mean values of the emitted gases.

		CO_2, g	**H_2, g**	**HF, g**
Set-up 1	*Average*	215,2	3,0	<0,1
	Std.Dev.	3,0	0,0	—
Set-up 2	*Average*	543,8	5,4	<0,1
	Std.Dev.	90,9	1,3	—
Set-up 3	*Average*	212,7	2,1	<0,1
	Std.Dev.	4,7	0,1	—

The mean emission values were tabulated in Tab. 1. For the first and last set-up with one pouch battery cell, the carbon dioxide values are consistent, together with hydrogen. In second set-up, the amount of carbon dioxide is doubled corresponding to the two pouch cells being burned. Hydrogen concentrations were at the level of 10,000-12,000 ppm v/v, thus not exceeding lower flammability limit (4% v/v for H_2). Carbon dioxide peak value was 4,5% and for the hydrogen was approximately 11000 ppm CO_2 concentration of above 5% may cause already serious effects on human health such as development of hypercapnia and respiratory acidosis [43].

No hydrogen fluoride was recorded for all of the processes. This may be caused due to dilution with high air volume flow (160 l/s). The sole efficiency of dry sorbent injection (without dilution) could not be measured due to excessive temperature of the thermal runaway gases exceeding sensor limits (50°C). Instead the estimated performance of both dry sorbent injection and dilution of the gases for the HF removal is about 99% based on theoretical production of 193.6 mg/Wh [16], and for the CO_2 removal is about 89% based on the theoretical volume of carbon dioxide in pouch NMC cells of 36.6% [44].

Table 2: Maximum temperature rises recorded in testing set-up 1-3 for thermocouple T1-3.

	T1, °C	**T2, °C**	**T3, °C**
Set-up 1 - Tmax	545,3	158,3	100,4
Set-up 2 - Tmax	765,3	186,2	111,3
Set-up 3 - Tmax	756,4	220,7	135,1

Temperature measurement point were positioned above the cell (T1), before the filter (T2) and behind the filter (T3), see Fig. 4. The maximum values recorded in each testing set-up were shown in Tab. 2. The temperature recorded before the filter (158.3-220.7°C) exceeded the maximum temperature allowable for the bag filter (120°C). Bag filter after each testing series was replaced. Despite high volume flow (approx. 1600 m^3/h) and supply of the ambient air, the thermal runaway gas temperature was still relatively high after the filtration.

5 Conclusion

The paper presents the development process of the thermal runaway emissions aftertreatment system. It discusses lithium-ion battery safety concerns in form of thermal runaway, which may happen during the everyday service. During thermal runaway, a plethora of toxic gases is produced, posing significant danger in confined space fire scenarios. Lithium-ion battery fire requires state of art technology to be doused due to its chemical self-sustaining nature. The risk of such fire is minimised with the mandatory testing, that often include causing thermal runaway on purpose. This, however, again is bound to produce vast amounts of toxic substances, which should be filtered or purified.

Following sections characterise potential substances found in TR gas emissions and discusses the compounds in respect to the part of the cell (SEI layer, cathode, anode and electrolyte). The most dangerous compounds for a human found in TR emissions are carbon monoxide and dioxide, hydrogen and hydrogen fluoride. Their toxicity as well as effect on health vary, however all may be categorised as toxic at given concentration levels. Subsequent review of the cleaning methods presents a dry sorbent injection based on calcium hydroxide as a possible solution for the gaseous emissions. The TREAS prototype is developed and subjected to simulation tests, and then a series empirical tests.

Based on the foregoing results, the following conclusions were drawn.

1. Dry sorbent injection based on calcium hydroxide dosage of 1.8 g/s and volume flow of approx. 1600 m^3/h may be used for filtration of the thermal runaway gas emissions with estimated performance of 99% for hydrogen fluoride and 89% for carbon dioxide.
2. Air velocity of 5-7.5 m/s are sufficient to provide dry sorbent transfer and filtration of the emitted gases. Large leakage losses are caused due to sorbent hopper and waste funnel.
3. The average production per Wh for CO_2 and H_2 were 1060,3 mg and 11,8 mg respectively. The peak recorded values were 4,5% (CO_2) and 11000 ppm (H_2).
4. Pouch NCM cell of 220 Wh production of hydrogen did not exceed a lower flammability limit of 40000 ppm v/v.

5. Temperature of the TR gases with the flow level of approx. 1600 m^3/h were at minimum 100,4°C. The temperature of the gas above the burning cells were at maximum 765,3°C.

Acknowledgements

The research was carried out within the fourth edition of the Program of the Polish Ministry of Science and Higher Education entitled "Doktorat wdrożeniowy" (Industrial Doctoral Program).

Received in June 2023

References

[1] X. Feng, M. Ouyang, X. Liu, L. Lu, Y. Xia, and X. He, "Thermal runaway mechanism of lithium ion battery for electric vehicles: A review," *Energy Storage Materials*, vol. 10, pp. 246–267, 2018.

[2] M. Ahrens, "Vehicle fires 2020," report, National Fire Protection Association, 2020.

[3] Deloitte, "2020 global automotive consumer study," report, Deloitte, 2020. [Online; accessed 14 February 2022].

[4] D. Darnikowski, M. Mieloszyk, and M. Weryk, "Fire resistance of construction elements," in *Sensors and Smart Structures Technologies for Civil, Mechanical, and Aerospace Systems 2022*, vol. 12046, pp. 203–218, SPIE, 2022.

[5] A. Dorsz and M. Lewandowski, "Analysis of fire hazards associated with the operation of electric vehicles in enclosed structures," *Energies*, vol. 15, p. 11, Dec 2021.

[6] Y. Chen, Y. Kang, Y. Zhao, L. Wang, J. Liu, Y. Li, Z. Liang, X. He, X. Li, N. Tavajohi, and B. Li, "A review of lithium-ion battery safety concerns: The issues, strategies, and testing standards," *Journal of Energy Chemistry*, vol. 59, pp. 83–99, 2021.

[7] H. Li, Q. Duan, C. Zhao, Z. Huang, and Q. Wang, "Experimental investigation on the thermal runaway and its propagation in the large format battery module with li (ni1/3co1/3mn1/3) o2 as cathode," *Journal of hazardous materials*, vol. 375, pp. 241–254, 2019.

[8] Q. Wang, P. Ping, X. Zhao, G. Chu, J. Sun, and C. Chen, "Thermal runaway caused fire and explosion of lithium ion battery," *Journal of power sources*, vol. 208, pp. 210–224, 2012.

[9] D. Darnikowski, "Fire resistance test methods of battery energy storage systems (bess): analysis, comparison and prospects," in *Selected Problems in Mechanical Engineering 2022* (M. Mieloszyk and T. Ochrymiuk, eds.), Gdansk, Poland: Wydawnictwo Instytutu Maszyn Przeplywowych PAN, 2022.

[10] A. Börger, J. Mertens, and H. Wenzl, "Thermal runaway and thermal runaway propagation in batteries: What do we talk about?," *Journal of Energy Storage*, vol. 24, p. 100649, 2019.

[11] M. Ghiji, V. Novozhilov, K. Moinuddin, P. Joseph, I. Burch, B. Suendermann, and G. Gamble, "A review of lithium-ion battery fire suppression," *Energies*, vol. 13, no. 19, 2020.

[12] C. Un and K. Aydın, "Thermal runaway and fire suppression applications for different types of lithium ion batteries," *Vehicles*, vol. 3, no. 3, pp. 480–497, 2021.

[13] S. Ubaldi, C. Di Bari, A. De Rosa, M. Michele, and P. Russo, "Investigation on effective fighting technology for lib fire," *Chemical Engineering Transactions*, vol. 91, pp. 505–510, 2022.

[14] D. Darnikowski and M. Mieloszyk, "Investigation into the lithium-ion battery fire resistance testing procedure for commercial use," *Batteries*, vol. 7, no. 3, p. 44, 2021.

[15] N. Omar, M. Daowd, O. Hegazy, G. Mulder, J.-M. Timmermans, T. Coosemans, P. Van den Bossche, and J. Van Mierlo, "Standardization work for bev and hev applications: Critical appraisal of recent traction battery documents," *Energies*, vol. 5, no. 1, pp. 138–156, 2012.

[16] F. Larsson, P. Andersson, P. Blomqvist, and B.-E. Mellander, "Toxic fluoride gas emissions from lithium-ion battery fires," *Scientific reports*, vol. 7, no. 1, pp. 1–13, 2017.

[17] E. C. for Europe of the United Nations, "Global technical regulation on the electric vehicle safety (evs)," regulation, Mar. 2016.

[18] "Regulation no 100 revision 02 - uniform provisions concerning the approval of vehicles with regard to specific requirements for the electric power train," tech. rep., Economic Commission for Europe of the United Nations, Aug. 2013.

[19] "Regulation no 100 revision 03 - uniform provisions concerning the approval of vehicles with regard to specific requirements for the electric power train," tech. rep., Economic Commission for Europe of the United Nations, Aug. 2021.

[20] "Electrically propelled road vehicles - Test specification for lithium-ion traction battery packs and systems - Part 3: Safety performance requirements," standard, International Organization for Standardization, Geneva, CH, May 2014.

[21] "Electrically propelled road vehicles - Safety specifications - Part 1: Rechargeable energy storage system (RESS)," standard, International Organization for Standardization, Geneva, CH, Apr. 2019.

[22] "Electrically propelled mopeds and motorcycles - Test specifications and safety requirements for lithium-ion battery systems," standard, International Organization for Standardization, Geneva, CH, Apr. 2017.

[23] "Electric and Hybrid Electric Vehicle Rechargeable Energy Storage System (RESS) Safety and Abuse Testing," standard, Society of Automotive Engineers, Warrendale, US, Apr. 2009.

[24] "Lithium-ion traction battery pack and system for electric vehicles - Part 3:Safety requirements and test methods," standard, Standardization Administration of the People's Republic of China, Shenzhen, CN, May 2015.

[25] "Recommended Practices for Abuse Testing Rechargeable Energy Storage Systems (RESSs)," standard, Sandia National Laboratories, Albuquerque, US, July 2017.

[26] "Batteries for Use In Electric Vehicles," standard, Underwriters Laboratories, Northbrook, US, Mar. 2020.

[27] L. Zhao, I. Watanabe, T. Doi, S. Okada, and J. ichi Yamaki, "Tg-ms analysis of solid electrolyte interphase (sei) on graphite negative-electrode in lithium-ion batteries," *Journal of Power Sources*, vol. 161, no. 2, pp. 1275–1280, 2006.

[28] H. Yang, H. Bang, K. Amine, and J. Prakash, "Investigations of the exothermic reactions of natural graphite anode for li-ion batteries during thermal runaway," *Journal of the Electrochemical Society*, vol. 152, no. 1, p. A73, 2004.

[29] G. Gachot, P. Ribière, D. Mathiron, S. Grugeon, M. Armand, J.-B. Leriche, S. Pilard, and S. Laruelle, "Gas chromatography/mass spectrometry as a suitable tool for the li-ion battery electrolyte degradation mechanisms study," *Analytical chemistry*, vol. 83, no. 2, pp. 478–485, 2011.

[30] B. Mao, H. Chen, Z. Cui, T. Wu, and Q. Wang, "Failure mechanism of the lithium ion battery during nail penetration," *International Journal of Heat and Mass Transfer*, vol. 122, pp. 1103–1115, 2018.

[31] X. Feng, X. He, M. Ouyang, L. Lu, P. Wu, C. Kulp, and S. Prasser, "Thermal runaway propagation model for designing a safer battery pack with 25 ah linixcoymnzo2 large format lithium ion battery," *Applied energy*, vol. 154, pp. 74–91, 2015.

[32] H. Arai, M. Tsuda, K. Saito, M. Hayashi, and Y. Sakurai, "Thermal reactions between delithiated lithium nickelate and electrolyte solutions," *Journal of The Electrochemical Society*, vol. 149, no. 4, p. A401, 2002.

[33] J. Li, Z. Zhang, X. Guo, and Y. Yang, "The studies on structural and thermal properties of delithiated lixni1/3co1/3mn1/3o2 (0 ¡ x ? 1) as a cathode material in lithium ion batteries," *Solid State Ionics*, vol. 177, no. 17-18, pp. 1509–1516, 2006.

[34] P. Ping, D. Kong, J. Zhang, R. Wen, and J. Wen, "Characterization of behaviour and hazards of fire and deflagration for high-energy li-ion cells by over-heating," *Journal of Power Sources*, vol. 398, pp. 55–66, 2018.

[35] A. Nedjalkov, J. Meyer, M. Köhring, A. Doering, M. Angelmahr, S. Dahle, A. Sander, A. Fischer, and W. Schade, "Toxic gas emissions from damaged lithium ion batteries - analysis and safety enhancement solution," *Batteries*, vol. 2, no. 1, p. 5, 2016.

[36] V. Somandepalli, K. Marr, and Q. Horn, "Quantification of combustion hazards of thermal runaway failures in lithium-ion batteries," *SAE International Journal of Alternative Powertrains*, vol. 3, no. 1, pp. 98–104, 2014.

[37] A. W. Golubkov, D. Fuchs, J. Wagner, H. Wiltsche, C. Stangl, G. Fauler, G. Voitic, A. Thaler, and V. Hacker, "Thermal-runaway experiments on consumer li-ion batteries with metal-oxide and olivin-type cathodes," *Rsc Advances*, vol. 4, no. 7, pp. 3633–3642, 2014.

[38] A. Dal Pozzo, R. Moricone, A. Tugnoli, and V. Cozzani, "Experimental investigation of the reactivity of sodium bicarbonate toward hydrogen chloride and sulfur dioxide at low temperatures," *Industrial & Engineering Chemistry Research*, vol. 58, no. 16, pp. 6316–6324, 2019.

[39] G. Hunt and M. Sewell, "Utilizing dry sorbent injection technology to improve acid gas control," in *Air and Waste Management Association - International Conference on Thermal Treatment Technologies and Hazardous Waste Combustors*, pp. 144–156, 2015.

[40] Y. Kong and H. Davidson, "Dry sorbent injection of sodium sorbents for so2, hcl and mercury mitigation," in *North American Waste-to-Energy Conference*, vol. 43932, pp. 317–320, 2010.

[41] R. K. Srivastava, W. Jozewicz, and C. Singer, "So2 scrubbing technologies: a review," *Environmental Progress*, vol. 20, no. 4, pp. 219–228, 2001.

[42] D. Schmal, A. Ligtvoet, and A. Brunia, "Some physico-chemical aspects of dry sorbent injection for removal of hci and hf from waste incinerator flue gases," *JAPCA*, vol. 39, no. 1, pp. 55–57, 1989.

[43] P. Parandoush and D. Lin, "A review on additive manufacturing of polymer-fiber composites," *Composite Structures*, vol. 182, pp. 36–53, 2017.

[44] T. Cai, P. Valecha, V. Tran, B. Engle, A. Stefanopoulou, and J. Siegel, "Detection of li-ion battery failure and venting with carbon dioxide sensors," *eTransportation*, vol. 7, p. 100100, 2021.